Talanta 126 (2014) 136–144

Contents lists available at ScienceDirect

Talanta

journal homepage: www.elsevier.com/locate/talanta

The effects of lipids and surfactants on TLR5-proteoliposome functionality for flagellin detection using surface plasmon resonance biosensing

Y. Olguín [a,*], L.G. Carrascosa [b], L.M. Lechuga [b], M. Young [a]

[a] Biotechnology Center, Federico Santa Maria Technical University, Valparaíso, Chile
[b] Nanobiosensor and Bioanalytical Applications Group, Institut Catàla de Nanociencia i Nanotecnología (ICN2), CSIC and CIBER-BBN, Bellaterra, Barcelona, Spain

ARTICLE INFO

Article history:
Received 16 December 2013
Received in revised form
25 March 2014
Accepted 27 March 2014
Available online 3 April 2014

Keywords:
Toll-like receptor 5
Proteoliposomes
Flagellin
Surface plasmon resonance

ABSTRACT

The use of proteoliposomes as affinity elements in conjunction with a surface plasmon resonance sensor is a high-sensitivity alternative for the detection of multiple analytes. However, one of the most important aspects of these conformations is maintaining the functionality of the immobilized protein, which is determined by the choice of lipids and surfactants employed in the reconstitutions.

Previously, we demonstrated the functionality of TLR5-proteoliposomes as screening affinity elements of bacterial flagellin. In this new study we change the conditions of immobilization of TLR5 and evaluate how the fluidity of the membrane and the final size of the liposomes affect the functionality of the construct and thus increase their utility as an affinity element for design of new biosensors.

In particular, we used reconstructions into preformed liposomes composed of the lipids POPC, POPC–DMPC and POPC–POPE mediated by the use of surfactants OG, Triton X100, and DDM, respectively. The affinity results were evaluated by SPR technology proteoliposomes and were correlated with the anisotropic change in the membrane status; the final sizes of the proteoliposomes were estimated.

Our results clearly show the dependence of fluidity and final size of the proteoliposomes with surface plasmon resonance affinity measurements.

1. Introduction

Affinity biosensors use different recognition elements that specifically interact with their corresponding ligands [1]. These elements, typically antibodies, enzymes, or genetic material, in combination with a transducer provide the necessary sensitivity for the evaluation of substances using biosensors [2]. However, despite their inherent qualities of physiological function, membrane proteins are not usually considered for use as recognition elements due to concerns of instability and functionality maintenance [3].

Nonetheless, as there is sufficient evidence of successful immobilizations and the analytical use of membrane proteins, it is possible to develop new criteria for considering membrane proteins as recognition elements for the development of novel biosensors [3–11]. Indeed, many disease agents and intoxicants that depend on interactions between a ligand and a membrane protein, such ion channels or immune recognition proteins, could be used to generate generic or specific biosensors [12–16]. Various systems have been used as transducers for the read-out of the biointeraction with the ligands, and one of the most prominents are the optical transducers based on Surface Plasmon Resonance (SPR), which allow for the immobilization of diverse recognition elements, including lipid formulations that can contain membrane proteins, with greater sensitivity over other systems [6,17–19].

Moreover, one of the most active areas in the development of biosensors is the detection of biological contaminants in water, particularly bacterial enteropathogens [20–23]. Outbreaks associated with intestinal infections generate large economic losses globally and result in massive control efforts to reduce clinical-level notification [24]. These situations have led to numerous investigations into generating biosensors for the detection of bacteria, mainly from the genera Escherichia, Salmonella, Vibrio, Clostridium, and Listeria [25–31].

A distinctive feature of these bacterial genera corresponds to their mobility due to the presence of flagella, pathogenic components that are detected by the host through the membrane protein TLR5 present on several cell types [32,33]. TLR5 specifically

* Correspondence to. Centro de Biotecnología. Universidad Técnica Federico Santa María. Avenida España 1680, Valparaíso, Chile. Tel.: +56 32 2654730; fax: +56 32 2654836.
E-mail address: yusser.olguin@postgrado.usm.cl (Y. Olguín).

http://dx.doi.org/10.1016/j.talanta.2014.03.065
0039-9140/

interacts with flagellin, the structural protein of the flagellum filament; this interaction triggers a series of events that results in the activation of the adaptive immune system and the removal of the infectious agent [34,35]. TLR5 has been shown to be useful as an analytical recognition element for low concentrations of flagellin, which alone represents a major immunogenic agent [36–38]. The sensitivity of devices that use TLR5 as the recognition element depends on the activity of the immobilized protein and the characteristics of the transducer [37].

In this regard, testing with functional recombinant human TLR5 produced in insect cells and immobilized in proteoliposomes has proven to be effective for detecting interactions with its ligand using surface plasmon resonance [37]. Regardless, there is a need to increase the sensitivity of TLR5-proteoliposomes, which requires the further exploration of immobilized protein stability, orientation, and dimerization in the liposome, and to determine how the system in which the protein is immobilized affects the sensitivity of the transducer [39].

The functionality of membrane proteins immobilized in lipid systems depends on several factors, including the type of lipid, type of surfactant, molar ratio of lipid/surfactant, and efficiency of surfactant removal [40–43]. The interaction of the lipid with the membrane protein is essential to promote the proper orientation and dimerization, which influences the functioning of the protein, particularly for TLR5, which also requires dimerization [43–45].

The order of the bilayer after reconstitution of the membrane protein represents a significant parameter that affects the functionality of the protein and can be measured by changes in the anisotropy of the bilayer [46]. Moreover, the surfactant may have an effect on the final size of the proteoliposome, which would influence the protein functionality and capability of the transducer when using a SPR transducer system [47,48].

To obtain a proteoliposome with a high affinity for flagellin, we investigated the immobilization conditions of TLR5 by varying the lipids and surfactants used in the reconstitution and how these modifications affect the affinity of TLR5-proteoliposomes. These results were correlated with the structural changes of the bilayer by measuring the variations of anisotropy and the final size of each conformation were used to obtain useful information on the generation of a flagellin biosensor using TLR5-proteoliposomes.

2. Experimental procedures

2.1. Materials

1-Palmitoyl-2-oleoyl-sn-glycero-3-phosphocholine (POPC), 1,2-dimyristoyl-sn-glycero-3-phosphocholine (DMPC), 1-palmitoyl-2-oleoyl-sn-glycero-3-phosphoethanolamine (POPE), and phytosphingosine of the highest purified grade were purchased from Avanti Polar Lipids Inc. (Birmingham, AL, USA). *n*-Dodecy-lβ-D-maltoside (DDM) and *n*-octyl-β-D-glucopyranoside (OG) were purchased from Calbiochem® (San Diego, CA, USA). Triton X-100 was purchased from Sigma-Aldrich Co. (St. Louis, MO, USA), and SM2 Bio-Beads® were purchased from Bio-Rad (Hercules, CA, USA). *N*-hydroxysuccinimide (NHS), 2-(*N*-morpholino) ethane sulfonic acid (MES) buffer, and *N*-ethyl-*N*′-(dimethylaminopropyl) carbodiimide hydrochloride (EDC · HCl) were purchased from Sigma-Aldrich Co. All other reagents were obtained from commercial sources. Recombinant TLR5 and flagellin (from *Escherichia coli*) were obtained using established protocols [37,49–51].

2.2. Liposome and proteoliposome preparation

For liposome formation, three lipid conformations, POPC, POPC:DMPC (1:1), and POPC:POPE (1:3), were used at an initial concentration of 10 μM, formed by solubilization with a mixture of chloroform:methanol (1:1, v/v), dried under a stream of nitrogen, and kept under high vacuum for 12 h. Multilamellar liposomes (MLVs) were obtained after dispersion of the film in 50 mM KPi buffer (buffer (K_2PO_4 1 M, $KHPO_4$ (1 M)) (pH 7.4) and vortexing above the transition-phase temperature (room temperature). The MLV suspensions were sonicated in an ultrasonic bath for 30 min and kept at 4 °C overnight to obtain unilamellar liposomes (LUVs).

For micelle (lipid–surfactant) formation, surfactants, 0.06% w/v DDM, 2% w/v OG, or 0.2% w/v Triton X100, were added to LUVs.

TLR5 (1.5 μM) was reconstituted by agitation of the mixture of solubilized protein with surfactant and micelles (lipids–surfactants) during 30 min at 4 °C to obtain mixed micelles (TLR5–lipid–surfactant). Proteoliposomes then were obtained by surfactant strip phase, adding polystyrene Bio-Beads SM2 and stirring the mixture at 25 °C for 2 h. After centrifugation at 12.000 × *g* for 1 h, the resulting pellet was resuspended in KPi buffer (pH 7.4), with a controlled increase in temperature up to 37 °C [52]. The TLR5 concentration in the proteoliposomes was performed by a modified Bradford assay [53,54], the surfactant and lipids concentration were determined spectroscopically (results are expressed as means and standard deviations of triplicate measurements) [55–57]. The size distribution of the liposomes and proteoliposomes was determined by a dynamic light scattering analysis (DLS) using a Zetasizer Nano ZS (Malvern Instruments, Worcestershire, UK) in triplicate at 25 °C for 60 s, with an average count rate of 280 kcps [58].

2.3. SPR device

The SPR evaluations were done using an in-lab-designed biosensor, as described elsewhere [59]. The device operates using a standard Kretschmann configuration in which the binding events are registered in real time by evaluating the variation in the intensity of the light reflected from a fixed angle [59]. The immobilization of the proteoliposomes onto gold sensor chip was performed using an in situ method [60]. Chip functionalization was done in three steps using previously activated sensor chip. The first step involved treatment with 40 mg/mL EDC and 10 mg/mL NHS for 10 min; the second step was performed with 0.5 mg/mL phytosphingosine dissolved in DMSO and sodium acetate (pH 5.2). In the third step, the proteoliposomes were added (total 1 mM lipid) for 25 min, followed by washing with 50 mM NaOH for 1 min [37]. The non-specific binding sites were blocked by adding 100 μL of 0.1 mg/mL BSA. After each measurement, the chip was regenerated with 40 mM CHAPS for 3 min, followed by 50 mM NaOH for 1 min, allowing the chip to be used five times [37].

2.4. SPR data analysis

The SPR results of the overall interactions were analyzed by nonlinear fitting to a pseudo first-order reaction model given by Eqs. (1) and (2). The interaction capture data analysis was performed using Origin 8.0 and graphing software. In Eq. (1), R_t is the SPR response at time t, R_{t0} is the response at time t_0, and kd is the dissociation rate constant.

$$R_t = R_{t0} e^{-kd(t-t_0)} \tag{1}$$

The association rate constant (k_a) is determined by Eq. (2), where R_{max} is the maximum response (proportional to the amount of immobilized ligand) and C is the concentration of analyte in solution. The affinity constants (expressed as K_D) for each system were calculated from the ratio of k_d/k_a [61].

$$R_t = \frac{k_a C R_{max}(1 - e^{-(k_a C + k_d)t})}{k_a C + k_d} \tag{2}$$

2.5. Steady-state anisotropy experiments

Assays by fluorescence anisotropy (r) were performed with the probe DPH (1,6-phenyl-1,3,5-hexatriene) (excitation wavelength of 350 nm and emission wavelength of 450 nm) incorporated into the liposome (1:700). The emission fluorescence was measured every 10 min throughout the reconstitution [62,63].

Furthermore, the transition (T_m) temperature for the liposomes comprised of the lipids POPC and POPC–DMPC–POPE was determined by measuring the changes in fluorescence anisotropy as a function of temperature increase using the DPH probe [64].

2.6. Statistical data analysis

For fluorescence anisotropy measurements, for a total of four experiments for each conformation, the data were expressed by Box plot 25.75, where a rectangular box with edges determined by the lower and upper quartiles, the median denoted as a line segment splitting the rectangular box into two adjoining boxes, the small quadrate is the mean, a whisker (that is, a line segment) from Q1 (the first quartile, the 25th percentile) to the minimum and a whisker from Q3 (the third quartile, the 75th percentile) to the maximum. For calculating the Pearson correlations, sizes and anisotropy measurements were used from four independent experiments for each type of proteoliposome regarding the mean SPR measurements [65].

3. Results and discussion

3.1. Structural order of bilayers in proteoliposomes: Steady-state anisotropy experiments

The transition temperature (T_m) is a characteristic parameter for each lipid; however, when lipids are mixed, it is necessary to determine a new value for the mixture, which must be evaluated prior to the formation of liposomes and proteoliposomes [66]. In this study, we determined the T_m value for the lipids configurations POPE–POPC and POPC–DMPC using fluorescence anisotropy [46,67]. By relating absolute anisotropy (r) with temperature, the transition temperature corresponds to the midpoint of the transition between lamellar liquid-crystalline (or fluid), with low values of anisotropy, and ordered gel phase, with high anisotropy values, considering ΔT_r as the temperature range associated with the phase transition [68]. The results established T_m values of 20 °C and 11 °C for the POPE:POPC and POPC:DMPC configurations, respectively (Fig. 1).

The reconstitution of membrane proteins into preformed liposomes produces perturbations in the organization of the bilayer, and these modifications affect the degree of insertion and most likely the formation of undesirable conglomerates in the membrane [69]. The fluidity of a bilayer is a key factor in modulating the function of membrane proteins [70,71], and the effect of TLR5 insertion reduces resistance to the mobility of membrane components, increasing the probability that two molecules of TLR5 can interact with each other and homodimerize, promoting the interaction with flagellin [72]. The degree of fluidity is estimated by fluorescence anisotropy, a variable that is inversely related to the fluidity and organization of a lipid bilayer, which is based on the existence of transition moments for excitation and emission that are oriented in specific directions in the structure of the fluorophore. Anisotropy is affected by changes in the orientation of the fluorescent molecules due to rotational movement [73]. Steady-state fluorescence anisotropy (r) is defined by Eq. (3):

$$r = \frac{I_{VV} - I_{VH}G}{I_{VV} + 2I_{VH}G} \quad (3)$$

where I_{VV} and I_{VH} are the vertical and horizontal intensity of polarized radiation when the excitation radiation is polarized vertically. The parameter G is an instrumental correction factor defined by the ratio $G = I_{HV}/I_{HH}$, where I_{HV} and I_{HH} are the vertical and horizontal intensity of polarized radiation, when the excitation radiation is polarized horizontally [73].

In agreement with other authors, our results for the variations in anisotropy and therefore in membrane fluidity after TLR5 reconstitution showed a dependence on the lipid and type of surfactant used [69,74]. According to Fig. 2, anisotropy decreased sharply during the first 30 min of the reconstitution. This event was appreciable in all of the samples and was related to the temperature increase from 4 °C to 25 °C.

During reconstitution, the inclusion of the membrane protein induces disorder in the continuity of the bilayer, resulting in a decrease in anisotropy related to the degree of protein incorporation [69]. Moreover, the extraction of surfactant during the reconstitution process also exerts a significant impact on the anisotropy of the bilayer, depending upon the type of surfactant and the experimental conditions, with the temperature, molar ratio, and effective surfactant extraction being critical [40,75,76].

In general, Fig. 2 shows that, for all samples, the anisotropy decreases relative to the initial condition of the liposomes. However, the changes in the order of the bilayer for the TLR5-proteoliposome samples using surfactants DDM and Triton X100 were higher than with OG. During reconstitution, the surfactant is removed to reduce the surfactant concentration to at least below the critical micelle concentration (CMC), thereby forming the proteoliposome, though the residual surfactant in the bilayer may still interact with the lipids and TLR5 transmembrane region [48,69]. OG possesses a higher CMC than DDM and Triton X100, which indicates that there is likely to be a greater number of OG molecules remaining in the bilayer after surfactant removal, causing structural changes that favor lipid order.

The bilayer fluidity, which is inversely proportional to anisotropy, is also dependent on the physico-chemical characteristics of the lipids [42]. In our research, the proteoliposomes formed with only POPC showed a greater ability to form proteoliposomes with enhanced fluidity, similar to the POPC–DMPC combination; in contrast, the anisotropy of the proteoliposomes composed of POPE showed small variation with respect to the initial condition of the liposomes (Fig. 2). The order of the bilayer is the result of interactions between all of the components of the membrane, both hydrophilic and hydrophobic [77]. In general, fluidity is favored by the presence of lipids with short and unsaturated hydrocarbon chains, though the interaction of polar regions also has a major effect on the order of the bilayer. According to our findings, these interactions might result in a slight decrease in anisotropy for the POPE lipid, which has a lower topological polar surface area compared to lipids with phosphocholine compounds [78].

The importance of interactions of headgroup of the phospholipid lies the van der Waals interactions and hydrogen bonds established with neighboring molecules, in this case, the incorporation of PE (phosphatidylethanolamine headgroup) in the PC (phosphatidylcholine headgroup) membrane increasing the thickness of membrane and provides a conformation, where PE is located near the hydrocarbon chains of PC, where such interactions are established strong van der Waals forces and hydrogen-bonding decreasing membrane fluidity, background provided experimentally and by molecular dynamics [79–81].

Comparing the results in the final state of the proteoliposomes (Fig. 3), according to the surfactant used, the variations in anisotropy were not statistically significant in various proteoliposomes types, though a less anisotropy is shown in POPC and POPC–DMPC proteoliposomes. In proteoliposomes containing DMPC, the lower chain length induces a increase in the structural disorder of the

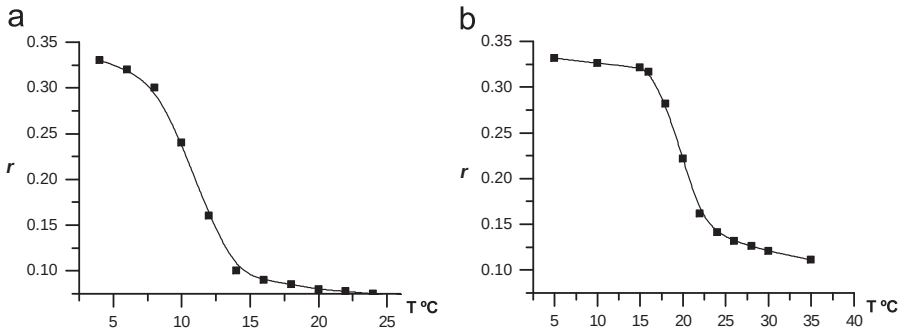

Fig. 1. T_m evaluation using fluorescence anisotropy. The T_m value of liposomes composed of the lipid mixtures POPC:DMPC (a) and POPC:POPE (b) was determined as the midpoint of the transition defined as ΔT_r.

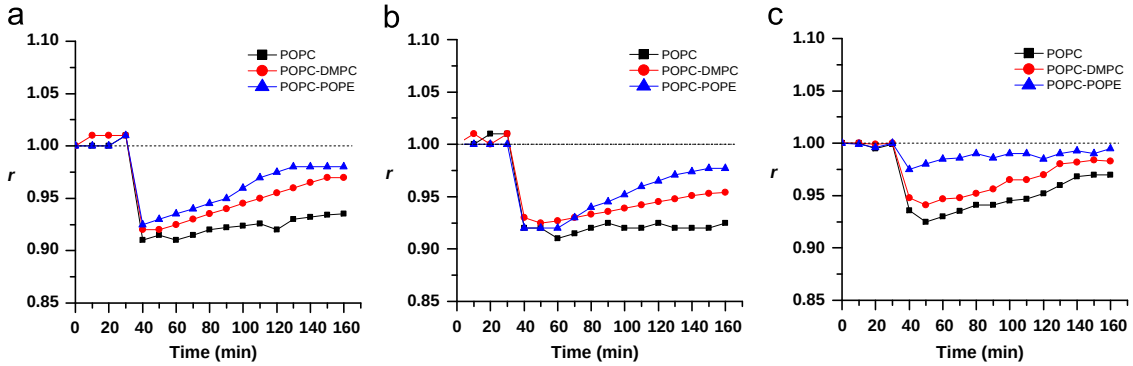

Fig. 2. Fluorescence anisotropy measurements. The lipid settings for each proteoliposome are shown in blue (POPC–POPE), red (POPC–DMPC), and black (POPC). Fluorescence (r) was measured every 10 min from time 0, corresponding to the state of anisotropy to the liposome prior to lipid disruption. The first point corresponds to the anisotropy reading of the liposome, until the 30 min corresponds to the mixture of the liposome and TLR5 solubilized with surfactants at 4 °C and the remaining points corresponds the stripping process of surfactant at 25 °C. The panels correspond to the surfactant used in the reconstitution process: DDM (a), Triton X100 (b), and OG (c). (each point represents the mean of the measurements ($n=4$)). (For interpretation of the references to color in this figure legend, the reader is referred to the web version of this article.)

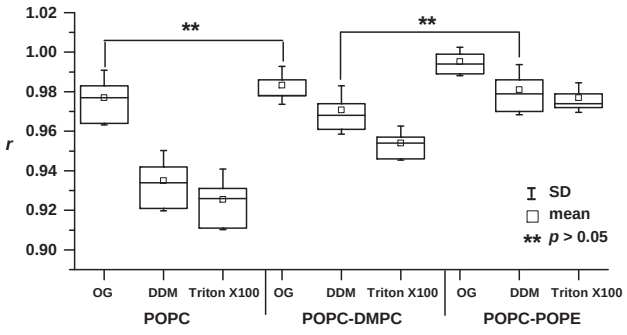

Fig. 3. Box plots for the final anisotropy state. Shown is the distribution of anisotropy results for the different configurations of proteoliposomes in the final state (arbitrarily set values, with approximately 1 corresponding to the initial state of anisotropy). The boxes represent percentile 25.75, the small quadrate is the mean, and the whiskers are standard deviations. The samples indicated with asterisks are not significantly different ($p > 0.05$).

membrane with resulting decreasing the anisotropy, generally lipids with shorter chains are less rigid due to more susceptibility to changes in kinetic energy and to their lower surface area, the stabilization by van der Waals forces exerted by neighboring chains is lower [82].

Regarding the membrane fluidity differences observed in the formation of proteoliposomes according the surfactants used, after reduction of detergent concentration below the CMC, the remaining surfactants into bilayer produce modifications of fluidity and permeability into proteoliposome depending on the structural characteristics of each molecule [83–85], which are correlated with the partition coefficient, the surface tension and the CMC of each detergent [86], which specifically has been able to correlate the partition coefficient and the CMC as a function of the ability of each surfactant to interact strongly with the lipid membranes, destabilizing the order of lipids it and consequently increasing membrane fluidity [87,88]. In this regard, various studies of structural analysis of the surfactants show that both the partition coefficient as CMC depends on the length of the alkyl chain, the shape and size of the molecule, the presence of heteroatoms and structural complexity [89–91]. For the surfactants used in this research, the values of CMC of OG (24–26 mM) are significantly higher than those that have been determined for DDM (0.15 mM) and Triton X100 (0.2–0.9 mM) respectively, while the partition coefficient (XLogP3-AA) of OG is the same as DDM (1.4) and lower than Triton X100 (4.6), these antecedents are consistent with of structural data, wherein the OG surfactant has a lower structural complexity and lower alkyl chain length, resulting in a lower affinity for membrane lipids compared with Triton X100 and DDM, consequently the fluidity in the state end of the TLR5-proteoliposomes is less when used OG in the reconstitution.

3.2. Characterization of TLR5-proteoliposome size and polydispersity

The final size of a proteoliposome is one of the important consequences of the reconstitution process of membrane proteins [92]. The formation of a relatively spherical bilayer includes the adoption of a structure equal to the amount of lipids in the outer and inner faces of the membrane; however, the inclusion of proteins into the membrane changes this relationship and

generates a new three-dimensional conformation to achieve structural stability [92].

The methodology used for the removal of the surfactant also affects the final size of the proteoliposome [93]. In general, the use of dialysis or gel filtration to remove the surfactant produces small proteoliposomes, unlike the case with the use of adsorbent materials. Upon reconstitution, the orientation of the reconstituted protein is dependent on the final size of the proteoliposome, and several studies demonstrate this condition as a key factor in the functionality of the transmembrane protein in the vesicle [43].

As observed in Fig. 4, the size distribution and polydispersity results are dependent on the surfactant and lipid used. Under our experimental conditions, the proteoliposomes resulting from the use of the OG surfactant were larger and showed a higher polydispersity compared to the proteoliposomes generated with DDM and Triton X100. OG has a shorter acyl chain, a high CMC, and binds strongly to the hydrophobic regions of the bilayer, properties that affect removal from the mixed surfactant–lipid–protein micelles and its relationship with the final size of the structure, resulting in large liposomes [69,94].

The characterization of the concentration ratio of each of the components of different proteoliposomes (Table 1) shows the effective incorporation of TLR5 in proteoliposomes with average percentage of 80% and varying concentrations of lipids and surfactants, which are not be statistically correlate with the effect on fluency, but rather to the structural characteristics of each component.

3.3. *Surface plasmon resonance experiments: Affinity tests*

Numerous investigations have shown the enormous potential and multifunctionality of surface plasmon resonance (SPR) to detect affinity [19]. However, as with other analytical techniques, its capacity becomes limited when used together with membrane proteins as biological recognition elements. This is mainly due to the technical difficulty of immobilization and the conservation of biological activity; in most cases, protein functionality is lost when using recombinant production systems [2].

The TLR5-proteoliposomes were immobilized on a sensor chip, and the activity was evaluated after the addition of flagellin into the system (100 μg/mL, extracted from *E. coli*) by calculating the kinetic dissociation and equilibrium dissociation constants for each reaction (Fig. 5).

Addition of flagellin to the immobilized proteoliposomes lead to a positive signal in all cases tested. The specificity of this detection system was analyzed by injecting blank (consisting only of liposomes, formed by the same lipids used in proteoliposomes) and control (BSA) samples showing no significant signal difference with the baseline. This result indicates that the immobilization approach was successful in maintaining TLR5 functionality promoting the selectively interaction of TLR5-proteoliposomes and flagellin, however with varying affinities depending on the conformation of lipid and surfactant, as shown in Figs. 5 and 6. Clearly, there was an effect of the surfactant used, particularly for the conformations with OG, where by the affinities of the proteoliposomes were lower than those using DDM and Triton X100. Specifically, OG reconstituted proteoliposomes showed less activity compared to the other conformations, with SPR values reaching approximately 32% of the value measured for the reconstituted DDM conformations and 44% for the Triton X100 conformations (Fig. 6).

Therefore, depending on the nature of the surfactant, three mechanisms can be identified by which the surfactant association with membrane proteins produces a functional proteoliposome: proteins can be either inserted into detergent-saturated liposomes, transferred from mixed micelles to detergent-saturated liposomes, or detergent participatio in proteoliposome formation during the micellar-to-lamellar transition [95]. These mechanisms

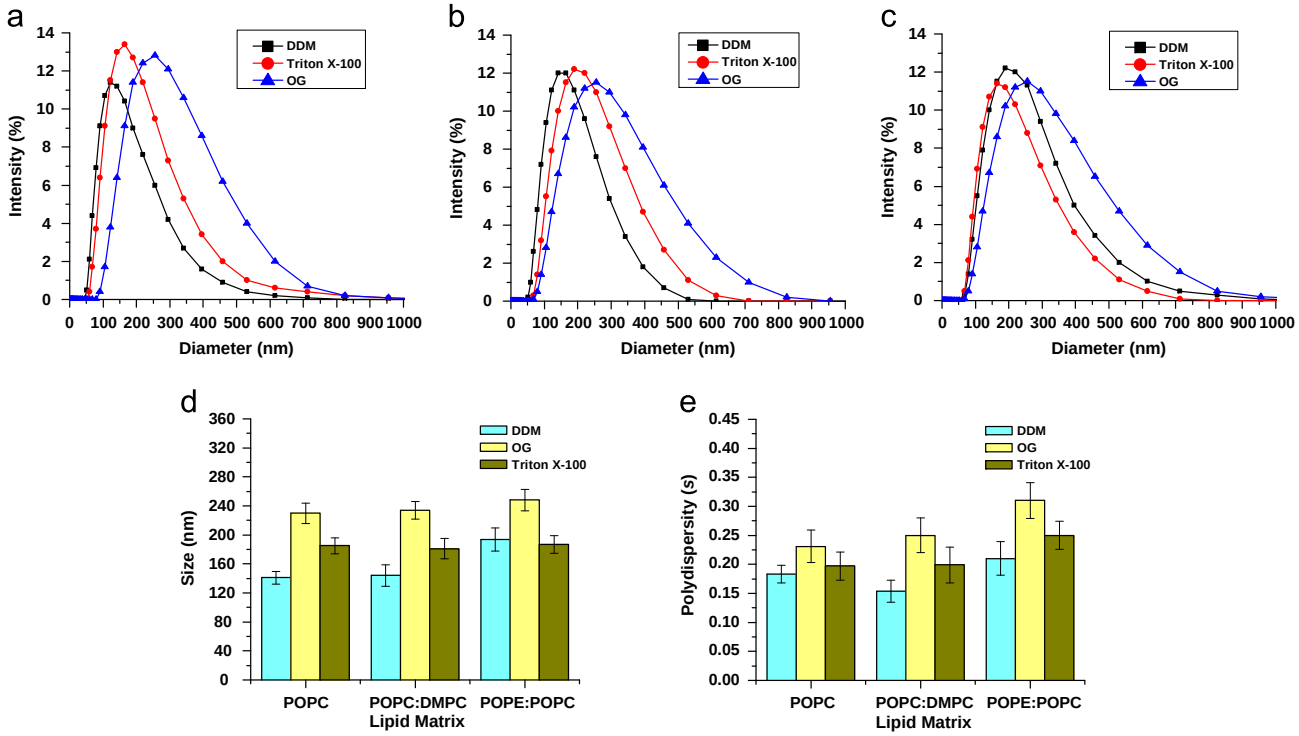

Fig. 4. Size and polydispersity of TLR5-proteoliposomes. Shown are size distribution curves according to the lipid matrix used. (a) POPC, (b) POPC–DMPC, and (c) POPC–POPE. (d) Summary bar graph of the average sizes according to the lipids used. (e) Bar graph showing the polydispersity of each sample. [(a) With kind permission from Springer Science+Business Media: <Analytical and Bioanalytical Chemistry, Detection of flagellin by interaction with human recombinant TLR5 immobilized in liposomes, 405, 2013, 1274, Y. Olguin, P. Villalobos, L.G. Carrascosa, M. Young, E. Valdez, L. Lechuga, R. Galindo in this figure.].

Table 1
Measurements of concentrations of lipid, surfactant, and Toll-like receptor 5 (TLR5) in mixed micelles and as part of proteoliposomes.

Lipid matrix	Surfactant	Initial			Final		
		Lipid (μM)	TLR5 (μM)	Surfactant (%w/v)	Lipid (μM)	TLR5 (μM)	Surfactant (%w/v)
POPC:DMPC	DDM	10	1.5	0.06	8.23 ± 0.08	1.23 ± 0.04	$6 \times 10^{-4} \pm 3 \times 10^{-5}$
	OG	10	1.5	2	9.68 ± 0.21	1.41 ± 0.06	$6.6 \times 10^{-3} \pm 7 \times 10^{-4}$
	Triton	10	1.5	0.2	9.09 ± 0.06	1.33 ± 0.14	$6.7 \times 10^{-3} \pm 7 \times 10^{-4}$
POPC	DDM	10	1.5	0.06	9.46 ± 0.02	1.29 ± 0.06	$3.9 \times 10^{-4} \pm 7 \times 10^{-5}$
	OG	10	1.5	2	9.51 ± 0.11	1.33 ± 0.09	$0.0079 \pm 6 \times 10^{-4}$
	Triton	10	1.5	0.2	9.41 ± 0.03	1.28 ± 0.23	$0.0041 \pm 8 \times 10^{-4}$
POPC:POPE	DDM	10	1.5	0.06	8.55 ± 0.07	1.12 ± 0.07	$7.4 \times 10^{-4} \pm 7 \times 10^{-5}$
	OG	10	1.5	2	9.78 ± 0.23	1.32 ± 0.08	$7.8 \times 10^{-3} \pm 8 \times 10^{-4}$
	Triton	10	1.5	0.2	9.66 ± 0.08	1.20 ± 0.1	$5.1 \times 10^{-3} \pm 8 \times 10^{-4}$

[(POPC data) With kind permission from Springer Science+Business Media: < Analytical and Bioanalytical Chemistry, Detection of flagellin by interaction with human recombinant TLR5 immobilized in liposomes, 405, 2013, 1276, Y. Olguin, P. Villalobos, L.G. Carrascosa, M. Young, E. Valdez, L. Lechuga, R. Galindo, Table 1].

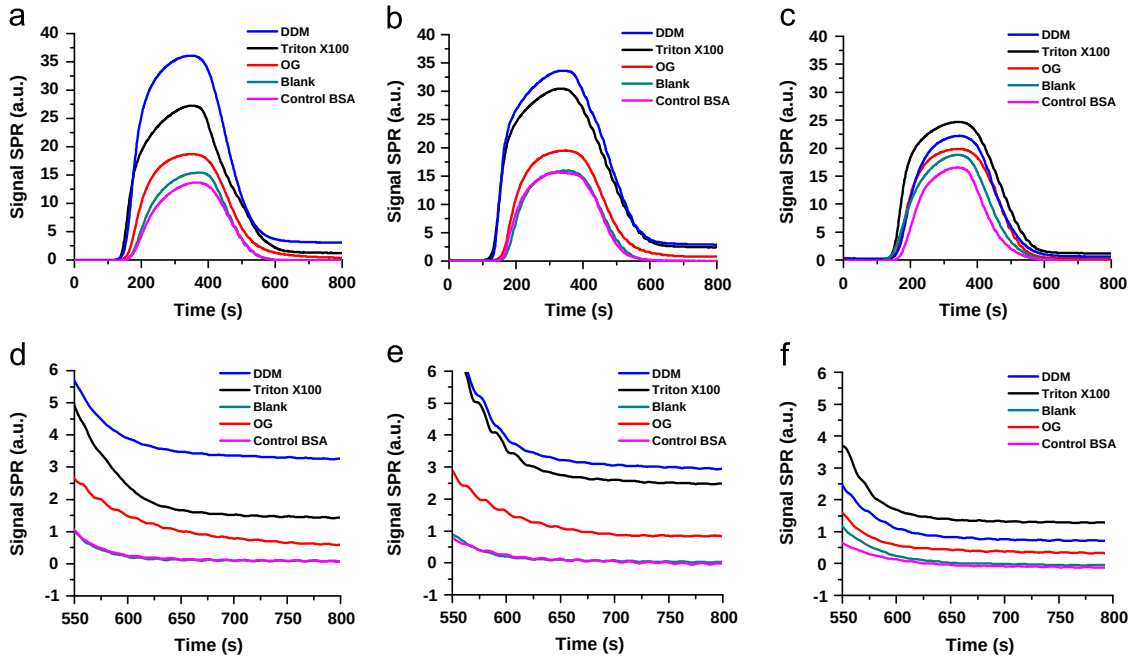

Fig. 5. SPR measurements of the interaction between flagellin and TLR5-proteoliposomes. Representative sensorgrams of one of the three measurements considered for each conformation. Different configurations of the lipid matrix and surfactant. (a) POPC, (b) POPC–DMPC, and (c) POPC–POPE. Graphs (d), (e), and (f) correspond to the amplification in the equilibrium region of graphs (a), (b), and (c), respectively. The configurations according to the surfactant used in the entire process of reconstitution are shown with different colors: black (Triton X100), red (OG), blue (DDM), cyan (blank) and magenta (control BSA). [(a) With kind permission from Springer Science+Business Media: < Analytical and Bioanalytical Chemistry, Detection of flagellin by interaction with human recombinant TLR5 immobilized in liposomes, 405, 2013, 1275, Y. Olguin, P. Villalobos, L.G. Carrascosa, M. Young, E. Valdez, L. Lechuga, R. Galindo in this figure]. (For interpretation of the references to color in this figure legend, the reader is referred to the web version of this article.)

have been implicated in the ability of each surfactant to maintain the functional properties of the solubilized membrane proteins and the correct insertion into the proteoliposome, moreover, a series of record shows that surfactants mediate the mechanisms by reconstruction occurs, optimizing the packaging of the reconstituted protein toward the best conformation of the proteins in the membranes [96,97]. However, there is no consensus that these mechanisms fully explain the behavior of the system, with the structural characteristics of the membrane protein and lipids affecting the characteristics of the overall conformation. Thus, it is possible that, for certain conformations, there could be a positive or negative effect on the reconstructions using DDM [98,99] and Triton X100 [100] and ultimately OG, as it is believed that chain length adversely affects interactions with membrane proteins in the proteoliposome, decreasing the activity [101,102]. Other methodological considerations have been studied in terms of the capability of each surfactant to saturate or solubilize liposomes and the consequent formation of the lipid–surfactant mixed micelles prior to incorporation of the protein [93,103]. The solubility curves supply information concerning the kinetics of lipid–surfactant interactions, providing two important variables: the surfactant to lipid molar ratio (*Re*) and the normalized bilayer/aqueous phase partition coefficient (*K*). *Re* is related to the ability of the surfactant to be included in a bilayer, thus determining the effectiveness of solubilization, the curvature of the surface of the liposome, and the possible difficulty of removing the surfactant. *K* is related to the ability of a surfactant to form mixed micelles with lipids [40,75,104–106]. In this regard, it is known that the OG surfactant has a great ability to saturate and solubilize liposomes, differing from the other surfactants used in this

research; this feature can contribute to explaining the differences in affinities obtained by SPR due to increased interactions of OG with the lipids used [107].

Furthermore, the affinity constants determined from the curves in the sensograms (Table 2) show the highest affinity conformations for the lipids composed of POPC and POPC–DMPC, 10 times higher than the affinity for the POPC–POPE mixture. Irrespective of the lipid composition, the proteoliposomes reconstituted using the lower surfactant OG show affinity constants an order of magnitude lower compared to DDM and Triton X100, following a similar trend as the equilibrium observed with the SPR values.

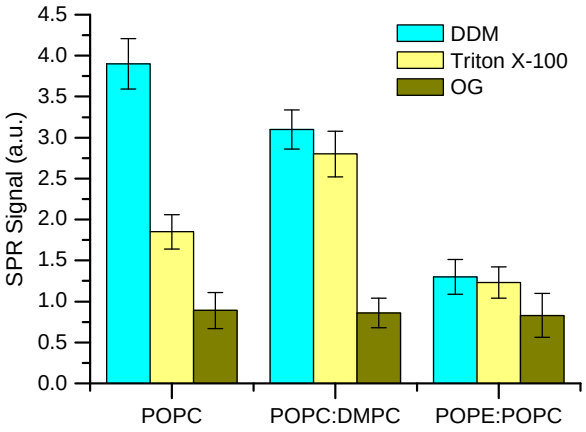

Fig. 6. SPR signal in the equilibrium region. The bar graph shows the signal in arbitrary units related to the baseline prior to the start of the interaction of flagellin with immobilized proteoliposomes. The graph is divided by the lipid matrix used; the surfactant used in each reconstitution is shown by colored bars. (For interpretation of the references to color in this figure legend, the reader is referred to the web version of this article.)

Table 2
Affinity constants determined by SPR. The affinity and dissociation constants determined from the SPR curves according to the lipids and surfactants used in each reconstitution are shown.

Lipid	Surfactant	K_d (s^{-1})	K_a ($M^{-1}s^{-1}$)	K_D (M)
POPC	DDM	$7\times10^{-3}(\pm8{,}3)$	$4.9\times10^{4}(\pm4{,}1)$	1.4×10^{-7}
	OG	$8\times10^{-3}(\pm4{,}0)$	$0.5810^{4}(\pm5{,}5)$	14×10^{-7}
	Triton X100	$9\times10^{-3}(\pm4{,}5)$	$1.1\times10^{4}(\pm2{,}1)$	8.2×10^{-7}
POPC–DMPC	DDM	$9\times10^{-3}(\pm4{,}7)$	$5.4\times10^{4}(\pm7{,}1)$	1.7×10^{-7}
	OG	$7.5\times10^{-3}(\pm4{,}7)$	$0.51\times10^{4}(\pm8{,}8)$	15×10^{-7}
	Triton X100	$8.7\times10^{-3}(\pm7{,}5)$	$1.8\times10^{4}(\pm3{,}1)$	4.8×10^{-7}
POPC–POPE	DDM	$8.1\times10^{-3}(\pm7{,}6)$	$0.74\times10^{4}(\pm6{,}2)$	11×10^{-7}
	OG	$7.1\times10^{-3}(\pm4{,}9)$	$0.55\times10^{4}(\pm5{,}9)$	13×10^{-7}
	Triton X100	$9\times10^{-3}(\pm5{,}5)$	$0.77\times10^{4}(\pm7{,}4)$	12×10^{-7}

[(POPC data) With kind permission from Springer Science+Business Media: < Analytical and Bioanalytical Chemistry, Detection of flagellin by interaction with human recombinant TLR5 immobilized in liposomes, 405, 2013, 1276, Y. Olguin, P. Villalobos, L.G. Carrascosa, M. Young, E. Valdez, L. Lechuga, R. Galindo, Table 1].

3.4. Correlations between size, anisotropy, and SPR responses

The activity of a proteoliposome is typically attributed to its particular characteristic structure, which can influence the affinity of the reconstituted protein. As shown in Fig. 7, the SPR responses were negatively correlated with anisotropy and the final size of the proteoliposome when the analysis was performed based on the lipid used in the reconstitution. In particular, there is an almost perfect dependence of the results for the lipid mixtures with the SPR responses and variation final anisotropy state (Fig. 7a).

The tendency was the same when the analysis was performed depending on the surfactant used, except for the OG surfactant; in this case, the data did not allow discrimination, resulting in a p-value > 0.05, with no statistical significance. For the same analysis according to the surfactant used, DDM and Triton X100 showed poor significant correlations with the SPR responses (Fig. 7b) though with the same trend in all conformations. Although there is evidence for a relationship between the final degree of anisotropy (inversely related to the fluidity) and the functionality of membrane proteins [76,108], increased fluidity does not necessarily imply an increase in activity of the reconstituted protein, as evidenced by the poor correlations between the affinity and conformations with POPC. Nevertheless, the conformation increased the affinity when complexed with the other lipids [109,110].

According our analysis, the final size of the proteoliposomes was strongly correlated with the affinity to flagellin. The final size of the proteoliposomes had two effects in our experiments. First, the structural relationship between the lipid bilayer, the final molar ratio lipid–protein, and the curvature adopted by the proteoliposome, which determine the particular three-dimensional position, has a direct influence on the activity of the protein [111]. Second, due to the characteristics of the electron evanescent wave, which is based on surface plasmon resonance, the distance from the gold surface where the interaction occurs determined the sensitivity of the measurement; thus, larger proteoliposomes provided lower SPR signals, this situation is correlatable with the results of the reconstructions of TLR5 with the surfactant OG, where sizes obtained are higher than those obtained using DDM or Triton X100 [17].

Despite extensive research relating to membrane proteins, only partial considerations of all phenomena involved in the activity of reconstituted protein have been considered, illustrating the uniqueness of each conformation, which is demonstrated by the inability to establish the magnitude of the all factors affecting activity [42,78,112–122]. In this regard, our results show the complex relationship between methodological variables and their impact on anisotropy and size, which are related to the affinity of

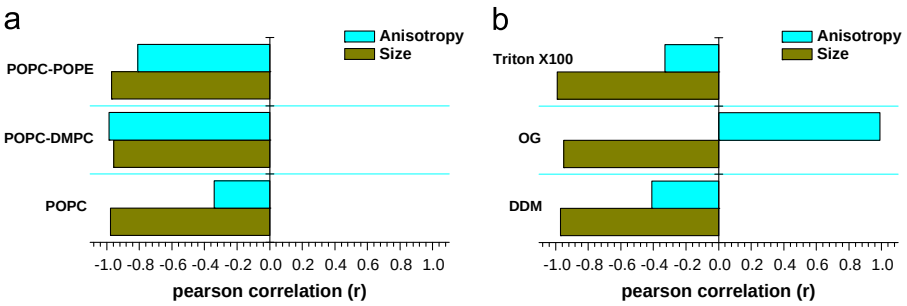

Fig. 7. Pearson correlations (r) as a function of SPR affinities. The bar graphs show the correlation as a function of the affinities measured in the region of equilibrium with respect to the lipids (a) and surfactants (b) used in the reconstructions.

TLR5 to flagellin, thereby providing a basis for the establishment of SPR biosensor-based TLR5-proteoliposomes.

Furthermore, this research demonstrates the high sensitivity of systems based on surface plasmon resonance (SPR) as transducers of proteoliposome interaction. The advantages of SPR systems over other label-free systems include simplicity and field use with high reproducibility. However, this study demonstrates a loss of sensitivity depending on the size of the proteoliposomes, a situation that could be overcome with the use of planar bilayers or immobilization in hydrogels [123,124].

4. Conclusion

The results of our research reveal that, despite the variability in the activity of proteoliposomes as a function of the experimental conditions, it is possible to construct biosensors based on the interaction of TLR5-flagellin.The activity of the resulting proteoliposomes can also be improved by optimizing the TLR5 reconstitution process. Using SPR biosensing, we found that the activity of the protein in liposomes can be manipulated by changing the lipids and surfactants used. POPC and the POPC–DMPC mixture reconstituted with DDM showed the best results enabling detection of flagellin levels up to 100 μg/mL. Conversely, based on our experimental conditions, OG surfactant and POPC–POPE lipid mixture were not suitable for promoting TLR5 activity and thus for the construction of flagellin biosensors.

Finally, the measurement of the final state of the bilayer anisotropy proves to be an important variable but is not as predictive of reconstituted TLR5 activity, as the measurement of the final size of the proteoliposomes, which is closely related to the activity of reconstituted TLR5.

Acknowledgments

Funding from Silob Chile Ltda., the Universidad Tecnica Federico Santa María (USM) and CONICYT through Fondef Project D07i1057. We also thank Juan Carlos Espinosa (University of Valparaíso)

References

[1] K.R. Rogers, Mol. Biotechnol. 14 (2000) 109–129.
[2] J.P. Chambers, B.P. Arulanandam, L.L. Matta, A. Weis, J.J. Valdes, Curr. Issues. Mol. Biol. 10 (2008) 1–12.
[3] J. Rucker, C. Davidoff, B.J. Doranz, Methods Mol. Biol. 617 (2010) 445–456.
[4] S. Basheer, D. Samyn, M. Hedstrom, M.S. Thakur, B.L. Persson, B. Mattiasson, Biosens. Bioelectron. 27 (2011) 58–63.
[5] A. Calò, M. Sanmartí-Espinal, P. Iavicoli, M.A. Persuy, E. Pajot-Augy, G. Gomila, J. Samitier, Soft Matter 8 (2012) 11632–11643.
[6] T. Christopeit, G. Stenberg, T. Gossas, S. Nystrom, V. Baraznenok, E. Lindstrom, U.H. Danielson, Anal. Biochem. 414 (2011) 14–22.
[7] B. Klee, E. John, F. Jähnig, Sens. Actuators, B 7 (1992) 376–379.
[8] P. Seelheim, H.J. Galla, Biochem. Biophys. Res. Commun. 431 (2013) 519–523.
[9] P. Seelheim, M. Seifert, G. H.J., Biophys. J. 98 (2010) 684a–685a.
[10] B. Vega, A. Calle, A. Sanchez, L.M. Lechuga, A.M. Ortiz, G. Armelles, J.M. Rodriguez-Frade, M. Mellado, Talanta 109 (2013) 209–215.
[11] B. Vega, L.M. Munoz, B.L. Holgado, P. Lucas, J.M. Rodriguez-Frade, A. Calle, J.L. Rodriguez-Fernandez, L.M. Lechuga, J.F. Rodriguez, R. Gutierrez-Gallego, M. Mellado, J. Leukocyte Biol. 90 (2011) 399–408.
[12] B. Billen, F. Bosmans, J. Tytgat, Curr. Pharm. Des 14 (2008) 2492–2502.
[13] T. Hayashi, T. Nakamura, A. Takaoka, Nihon Rinsho Meneki Gakkai Kaishi 34 (2011) 329–345.
[14] R. Medzhitov, Nat. Rev. Immunol. 1 (2001) 135–145.
[15] M.H. Rashid, S. Mahdavi, S. Kuyucak, Mar. Drugs 11 (2013) 848–869.
[16] H. Wang, F. Zhang, D. Li, S. Xu, J. He, H. Yu, J. Li, Z. Liu, S. Liang, Toxicon 65 (2013) 68–75.
[17] I. Abdulhalim, M. Zouro, A. Lakhtakiac, Electromagnetics 28 (2008) 214–242.
[18] P. Englebienne, A. Van Hoonacker, M. Verhas, Spectroscopy 17 (2003) (255-173).
[19] M. Piliarik, H. Vaisocherova, J. Homola, Methods Mol. Biol. 503 (2009) 65–88.
[20] P. Arora, A. Sindhu, N. Dilbaghi, A. Chaudhury, Biosens. Bioelectron. 28 (2011) 1–12.
[21] P. Leonard, S. Hearty, J. Brennan, L. Dunne, J. Quinn, T. Chakraborty, R. O'Kennedy, Enzyme Microb. Technol. 32 (2003) 3–13.
[22] M. Nayak, A. Kotian, S. Marathe, D. Chakravortty, Biosens. Bioelectron. 25 (2009) 661–667.
[23] V. Velusamy, K. Arshak, O. Korostynska, K. Oliwa, C. Adley, Biotechnol. Adv. 28 (2010) 232–254.
[24] G.T. Keusch, O. Fontaine, A. Bhargava, C. Boschi-Pinto, Z.A. Bhutta, E. Gotuzzo, J. Rivera, J. Chow, S. Shahid-Salles, R. Laxminarayan, Diarrheal diseases, in: D. T. Jamison, J.G. Breman, A.R. Measham (Eds.), Disease Control Priorities in Developing Countries, World Bank, Washington (DC), 2006.
[25] S. Bok, V. Korampally, C.M. Darr, W.R. Folk, L. Polo-Parada, K. Gangopadhyay, S. Gangopadhyay, Biosens. Bioelectron. 41 (2013) 409–416.
[26] Y. Chai, S. Horikawa, S. Li, H.C. Wikle, B.A. Chin, Biosens. Bioelectron. 50 (2013) 311–317.
[27] S. Chattopadhyay, A. Kaur, S. Jain, H. Singh, Biosens. Bioelectron. 45 (2013) 274–280.
[28] S.R. Horner, C.R. Mace, L.J. Rothberg, B.L. Miller, Biosens. Bioelectron. 21 (2006) 1659–1663.
[29] J. Moon, G. Kim, S. Lee, S. Park, J. Microbiol. Methods 95 (2013) 162–166.
[30] H. Sharma, R. Mutharasan, Biosens. Bioelectron. 45 (2013) 158–162.
[31] J. Zhang, Z. Li, H. Zhang, J. Wang, Y. Liu, G. Chen, J. Microbiol. Methods 93 (2013) 37–41.
[32] E. Andersen-Nissen, K.D. Smith, R. Bonneau, R.K. Strong, A. Aderem, J. Exp. Med. 204 (2007) 393–403.
[33] S.E. Applequist, E. Rollman, M.D. Wareing, M. Liden, B. Rozell, J. Hinkula, H.G. Ljunggren, J. Immunol. 175 (2005) 3882–3891.
[34] J.C. Bambou, A. Giraud, S. Menard, B. Begue, S. Rakotobe, M. Heyman, F. Taddei, N. Cerf-Bensussan, V. Gaboriau-Routhiau, J. Biol. Chem. 279 (2004) 42984–42992.
[35] K.D. Smith, E. Andersen-Nissen, F. Hayashi, K. Strobe, M.A. Bergman, S.L. Barrett, B.T. Cookson, A. Aderem, Nat. Immunol. 4 (2003) 1247–1253.
[36] A.N. Honko, S.B. Mizel, Immunol. Res. 33 (2005) 83–101.
[37] Y. Olguin, P. Villalobos, L.G. Carrascosa, M. Young, E. Valdez, L. Lechuga, R. Galindo, Anal. Bioanal. Chem. 405 (2013) 1267–1281.
[38] H. Zeng, A.Q. Carlson, Y. Guo, Y. Yu, L.S. Collier-Hyams, J.L. Madara, A.T. Gewirtz, A.S. Neish, J. Immunol. 171 (2003) 3668–3674.
[39] A. Darszon, J. Bioenerg. Biomembr. 15 (1983) 321–334.
[40] S. Almog, B.J. Litman, W. Wimley, J. Cohen, E.J. Wachtel, Y. Barenholz, A. Ben-Shaul, D. Lichtenberg, Biochemistry 29 (1990) 4582–4592.
[41] W. Dowhan, M. Bogdanov, Biochem. Soc. Trans. 39 (2011) 767–774.
[42] A.G. Lee, Biochim. Biophys. Acta 2003 (1612) 1–40.
[43] J.L. Rigaud, D. Levy, Methods Enzymol. 372 (2003) 65–86.
[44] J. Lu, P.D. Sun, Sci. Signal 5 (2012) (pe11).
[45] Y.G. Zhu, J.M. Qu, Chin. Med. J. 120 (2007) 56–61.
[46] B.M. Stott, M.P. Vu, C.O. McLemore, M.S. Lund, E. Gibbons, T.J. Brueseke, H.A. Wilson-Ashworth, J.D. Bell, J. Lipid Res. 49 (2008) 1202–1215.
[47] N.J. de Mol, M.J. Fischer, Methods Mol. Biol. 627 (2010) 1–14.
[48] A. González-Mancera, V. Kumar, M. Jamal, C. Eggleton, Effects of a surfactant monolayer on the measurement of equilibrium interfacial tension of a drop in extensional flow, J. Colloid Interface Sci. 333 (2009) 570–578.
[49] G.F. Ibrahim, G.H. Fleet, M.J. Lyons, R.A. Walker, J. Clin. Microbiol. 22 (1985) 1040–1044.
[50] H.S. Kim, S.D. Woo, W.J. Kim, J.Y. Choi, S.K. Kang, Cytotechnology 32 (2000) 87–92.
[51] D.F. Tian, B. Hong, S.Y. Si, Biomed. Environ. Sci. 18 (2005) 265–272.
[52] S. Merino-Montero, O. Domenech, M.T. Montero, J. Hernandez-Borrell, Biophys. Chem. 119 (2006) 78–83.
[53] R.S. Kaplan, P.L. Pedersen, Methods. Enzymol. 172 (1989) 393–399.
[54] P.H. Weigel, Z. Kyossev, L.C. Torres, J. Biol. Chem. 281 (2006) 36542–36551.
[55] M. DuBois, K.A. Gilles, J.K. Hamilton, P.A. Rebers, F. Smith, Anal. Chem. 28 (1976) 350–356.
[56] L.S. Lagutina, K.F. Shol'ts, Prikl. Biokhim. Mikrobiol. 38 (2002) 341–344.
[57] J.C. Stewart, Anal. Biochem. 104 (1980) 10–14.
[58] M. Baez, R. Cabrera, V. Guixe, J. Babul, Biochemistry 46 (2007) 6141–6148.
[59] L.G. Carrascosa, S. Gomez-Montes, A. Avino, A. Nadal, M. Pla, R. Eritja, L.M. Lechuga, Nucleic Acids Res. 40 (2012) e56.
[60] J Treviño, A. Calle, J.M. Rodríguez-Frade, M. Mellado, L.M. Lechuga, Clin. Chim. Acta 403 (2009) 56–62.
[61] M.A. Cooper, A. Hansson, S. Lofas, D.H. Williams, Anal. Biochem. 277 (2000) 196–205.
[62] D. Schwarz, V. Kruger, A.A. Chernogolov, S.A. Usanov, A. Stier, Biochem. Biophys. Res. Commun. 195 (1993) 889–896.
[63] G.B. Bhat, E.R. Block, Am. J. Respir. Cell Mol. Biol. 6 (1992) 633–638.
[64] S. Merino, J. Vazquez, O. Domenech, M. Berlanga, M. Vinas, T. Montero, J. Hernandez-Borrel, Langmuir 18 (2002) 3288–3292.
[65] K. Keen, Graphics for Statistics and Data Analysis with R Chapman and Hall/CRC Boca Raton, 2010.
[66] J. Chen, D. Cheng, J. Li, Y. Wang, J.X. Guo, Z.P. Chen, B.C. Cai, T. Yang, Drug Dev. Ind. Pharm. 39 (2013) 197–204.
[67] S. Kitagawa, M. Sawada, H. Hirata, Int. J. Pharm. 98 (1993) 203–208.
[68] G.D. Bothun, B.L. Knutson, H.J. Strobel, S.E. Nokes, Langmuir 21 (2005) 530–536.
[69] P. Neves, S.C. Lopes, I. Sousa, S. Garcia, P. Eaton, P. Gameiro, J. Pharm. Biomed. Anal. 49 (2009) 276–281.
[70] M. Manna, C. Mukhopadhyay, PLoS One 8 (2013) e71308.
[71] H.M. Ulmer, H. Herberhold, S. Fahsel, M.G. Ganzle, R. Winter, R.F. Vogel, Appl. Environ. Microbiol. 68 (2002) 1088–1095.

[72] S. Bose, J. Feix, S. Seetharam, B. Seetharam, J. Biol. Chem. 271 (1996) 11718–11725.
[73] J.R. Lakowicz, Introduction to fluorescence, in: J.R. Lakowicz (Ed.), Principles of Fluorescence Spectroscopy, Springer, Baltimore, Maryland, 2006.
[74] B. Aricha, I. Fishov, Z. Cohen, N. Sikron, S. Pesakhov, I. Khozin-Goldberg, R. Dagan, N. Porat, J. Bacteriol. 186 (2004) 4638–4644.
[75] O. Lopez, M. Cocera, L. Coderch, J.L. Parra, A. de la Maza, Colloid Polym. Sci. 280 (2002) 252–257.
[76] T. Shimanouchi, H. Ishii, N. Yoshimoto, H. Umakoshi, R. Kuboi, Colloids Surf., B 73 (2009) 156–160.
[77] J.M. East, D. Melville, A.G. Lee, Biochemistry 24 (1985) 2615–2623.
[78] I.D. Pogozheva, S. Tristram-Nagle, H.I. Mosberg, A.L. Lomize, Biochim. Biophys. Acta. 2013 (1828) 2592–2608.
[79] S. Leekumjorn, A.K. Sum, Biophys. J. 90 (2006) 3951–3965.
[80] H.I. Petrache, S.W. Dodd, M.F. Brown, Biophys. J. 79 (2000) 3172–3192.
[81] K.J. Seu, L.R. Cambrea, R.M. Everly, J.S. Hovis, Biophys. J. 91 (2006) 3727–3735.
[82] B. Robert, Biomembranes, Robert, Springer Science+Business Media, New York, 1989 (B. ed.).
[83] A. de la Maza, J.L. Parra, Biophys. J. 72 (1997) 1668–1675.
[84] S.H. Donaldson Jr., C.T. Lee Jr., B.F. Chmelka, J.N. Israelachvili, Proc. Nat. Acad. Sci. U.S.A. 108 (2011) 15699–15704.
[85] H. Heerklotz, Rev. Biophys 41 (2008) 205–264.
[86] J. Hu, X. Zhang, Z. Wang, Int. J. Mol. Sci. 11 (2010) 1020–1047.
[87] H. Heerklotz, J. Seelig, Biophys. J 78 (2000) 2435–2440.
[88] D. Lichtenberg, H. Ahyayauch, A. Alonso, F.M. Goni, Trends Biochem. Sci. 38 (2013) 85–93.
[89] G. Catanoiu, E. Carey, S. Patil, S. Engelskirchen, C. Stubenrauch, J. Colloid Interface Sci. 365 (2011) 150–156.
[90] A. Katritzky, L. Pacureanu, S. Slavov, D. Dobchev, M. Karelson, Ind. Eng. Chem. Res. 47 (2008) 9687–9695.
[91] Z. Wang, D. Huang, S. Gong, G. Li, Chin. J. Chem. 21 (2003) 1573–1579.
[92] M.M. Parmar, K. Edwards, T.D. Madden, Biochim. Biophys. Acta 1421 (1999) 77–90.
[93] M. Yokogawa, K. Takeuchi, I. Shimada, J. Am. Chem. Soc. 127 (2005) 12021–12027.
[94] A.M. Seddon, P. Curnow, P.J. Booth, Biochim. Biophys. Acta 2004 (1666) 105–117.
[95] J.L. Rigaud, B. Pitard, D. Levy, Biochim. Biophys. Acta 1231 (1995) 223–246.
[96] J. Lasch, J. Hoffmann, W.G. Omelyanenko, A.A. Klibanov, V.P. Torchilin, H. Binder, K. Gawrisch, Biochim. Biophys. Acta 1022 (1990) 171–180.
[97] M.T. Paternostre, M. Roux, J.L. Rigaud, Biochemistry 27 (1988) 2668–2677.
[98] K.G. Fleming, A.L. Ackerman, D.M. Engelman, J. Mol. Biol. 272 (1997) 266–275.
[99] T. VanAken, S. Foxall-VanAken, S. Castleman, S. Ferguson-Miller, Methods. Enzymol. 125 (1986) 27–35.
[100] Y. Fang, Int. J. Electrochem. 2011 (2011) 14.
[101] S.K. Lee, A. Stack, E. Katzowitsch, S.I. Aizawa, S. Suerbaum, C. Josenhans, Microb. Infect. 5 (2003) 1345–1356.
[102] S. Lund, S. Orlowski, B. de Foresta, P. Champeil, M. le Maire, J.V. Moller, J. Biol. Chem. 264 (1989) 4907–4915.
[103] Y. Gohon, J. Popot, Curr. Opin. Colloid Interface Sci. 8 (2003) 15–22.
[104] J.G. Kim, J.D. Kim, J. Biochem. 110 (1991) 436–442.
[105] D. Lichtenberg, Biochim. Biophys. Acta 821 (1985) 470–478.
[106] T. Tsuchiya, S. Saito, J. Biochem. 96 (1984) 1593–1597.
[107] O. Lopez, M. Cocera, J.L. Parra, A. de la Maza, Colloids Surf. 193 (2001) 221–229.
[108] G. Lenaz, Biosci. Rep. 7 (1987) 823–837.
[109] L.E. Cybulski, D. de Mendoza, Curr. Protein Pept. Sci. 12 (2011) 760–766.
[110] S.S. Krishnamurthy, R. Prasad, FEMS Microbiol. Lett. 173 (1999) 475–481.
[111] J. Marcelino, J.L. Lima, S. Reis, C. Matos, Chem. Phys. Lipids 146 (2007) 94–103.
[112] N. Dan, S.A. Safran, Biophys. J. 75 (1998) 1410–1414.
[113] S.L. Keller, S.M. Bezrukov, S.M. Gruner, M.W. Tate, I. Vodyanoy, V.A. Parsegian, Biophys. J. 65 (1993) 23–27.
[114] J.A. Lundbaek, A.M. Maer, O.S. Andersen, Biochemistry 36 (1997) 5695–5701.
[115] H. Pain, Mechanisms of Protein Folding, Oxford University Press, Oxford, 2000.
[116] J. Payandeh, T. Scheuer, N. Zheng, W.A. Catterall, Nature 475 (2011) 353–358.
[117] D. Schmidt, Q.X. Jiang, R. MacKinnon, Nature 444 (2006) 775–779.
[118] A.W. Smith, Biochim. Biophys. Acta 2012 (1818) 172–177.
[119] A.A. Sobko, E.A. Kotova, Y.N. Antonenko, S.D. Zakharov, W.A. Cramer, FEBS Lett. 576 (2004) 205–210.
[120] W.E. Teague Jr., O. Soubias, H. Petrache, N. Fuller, K.G. Hines, R.P. Rand, K. Gawrisch, Faraday Discuss. 161 (2013) 383–395.
[121] F.I. Valiyaveetil, Y. Zhou, R. MacKinnon, Biochemistry 41 (2002) 10771–10777.
[122] J. Zimmerberg, M.M. Kozlov, Nat. Rev. Mol. Cell Biol. 7 (2006) 9–19.
[123] M.M. Dominguez, M. Wathier, M.W. Grinstaff, S.E. Schaus, Anal. Chem. 79 (2007) 1064–1066.
[124] M.L. Wagner, L.K. Tamm, Biophys. J. 79 (2000) 1400–1414.